Received: 27 December 2016 | Revised: 22 May 2017 | Accepted: 25 May 2017
DOI: 10.1002/ajmg.a.38343

ORIGINAL ARTICLE

WILEY AMERICAN JOURNAL OF medical genetics PART A

Automatic recognition of the XLHED phenotype from facial images

Smail Hadj-Rabia[1] | Holm Schneider[2] | Elena Navarro[3] | Ophir Klein[4] | Neil Kirby[5] | Kenneth Huttner[5,6] | Lior Wolf[7,8] | Melanie Orin[7] | Sigrun Wohlfart[2] | Christine Bodemer[1] | Dorothy K. Grange[9]

[1] Department of Dermatology, Reference center for genodermatoses and rare skin diseases (MAGEC), INSERM U1163, Université Paris Descartes—Sorbonne Paris Cité, Institut Imagine, Hôpital Universitaire Necker-Enfants Malades, Paris, France

[2] Competence Center for Ectodermal Dysplasias, Department of Pediatrics, University Hospital Erlangen, Erlangen, Germany

[3] Center for Biomedical Network Research on Rare Diseases (CIBERER), C/Alvaro de Bazan, 10 Bajo Valencia, Spain

[4] Departments of Orofacial Sciences and Pediatrics, Program in Craniofacial Biology, and Institute for Human Genetics, University of California San Francisco, San Francisco, California

[5] Edimer Pharmaceuticals Inc, Cambridge Pkwy, Cambridge, Massachusetts

[6] Novartis/NIBR/NIDU, Cambridge, Massachusetts

[7] FDNA Inc, Boston, Massachusetts

[8] Department of Computer Sciences, University of Tel Aviv, Ramat-Aviv, Tel Aviv-Jaffa, Israel

[9] Department of Pediatrics, Washington University School of Medicine, St. Louis, Missouri

Correspondence
Smail Hadj-Rabia, Service de Dermatologie, Hôpital Necker-Enfants Malades, 149 rue de Sèvres 75015 Paris, France.
Email: smail.hadj@inserm.fr

X-linked hypohidrotic ectodermal dysplasia (XLHED) is a genetic disorder that affects ectodermal structures and presents with a characteristic facial appearance. The ability of automated facial recognition technology to detect the phenotype from images was assessed . In Phase 1 of this study we examined if the age of male patients affected the technology's recognition. In Phase 2 we investigated how well the technology discriminated affected males cases from female carriers and from individuals with other ectodermal dysplasia syndromes. The system detected XLHED to be the most likely diagnosis in all genetically confirmed affected male patients of all ages, and in 55% of heterozygous females. Interestingly, patients with other ED syndromes were also detected by the XLHED-targeted analysis, consistent with shared developmental features. Thus the automated facial recognition system represents a promising non-invasive technology to screen patients at all ages for a possible diagnosis of ectodermal dysplasia, with greatest sensitivity and specificity for males affected with XLHED.

KEYWORDS
anhidrotic/hypohidrotic ectodermal dysplasia, automated facial recognition, dermatology, dysmorphology, pediatrics

1 | INTRODUCTION

Ectodermal dysplasia (ED) is a clinically and genetically heterogeneous condition characterized by abnormal development of two or more of the following ectodermal-derived structures: hair, teeth, nails, and sweat glands (Visinoni, Lisboa-Costa, Pagnan, & Chautard-Freire-Maia, 2009). To date, more than 186 different ED syndromes have been reported.

Hypohidrotic or anhidrotic ectodermal dysplasia (HED), the most common phenotype of ED, is characterized by a triad of signs

comprising sparse hair (hypotrichosis), abnormal or missing teeth (hypodontia or anodontia) and reduced or absent sweating ability (hypo- or anhidrosis). The most frequent form of HED results from mutations in the gene *EDA* (formerly *EDA1*, chromosome Xq12-q13.1) encoding ectodysplasin A (EDA). Mutations in the EDA receptor gene (*EDAR*, chromosome 2q13) and in the gene encoding the EDAR-associated death domain (*EDARADD*, chromosome 1q42-q43) have been shown to cause autosomal recessive and dominant forms of HED. These three forms are clinically indistinguishable, probably because they alter a single signal transduction in the NF-κB signaling pathway which is necessary for initiation, formation, and differentiation of skin appendages. Two other genes are involved in HED: *WNT10A* and *TRAF6* (Wisniewski & Trzeciak, 2012). Together, mutations in *EDA*, *EDAR*, *EDRADD*, and *WNT10A* genes account for 90% of patients with HED (Cluzeau et al., 2011).

Early diagnosis of HED is challenging in neonates. At birth, teeth, and hair are normally absent and the measurement of sweating remains difficult. Clinical variability is also observed among female carriers of XLHED, the phenotype of whom ranges from normal to severely affected (in very few of them) (Cambiaghi, Restano, Pääkkönen, Caputo, & Kere, 2000; Fete, Hermann, Behrens, & Huttner, 2014; Schneider et al., 2011). Until now, the absent or mild HED manifestation in females carrying *EDA* mutations has been ascribed to X-chromosome inactivation.

In addition to the classical clinical triad, XLHED patients exhibit typical facial features as shown by 3D imaging and morphometrics: narrow, short face, long, prominent chin, narrow nose with a pinched tip, high zygomatic arches, short philtrum, midface retrusion, thick lower lip vermillion, prognathism, and narrow mouth (Goodwin et al., 2014). This typical facial phenotype is less obvious in XLHED females (Saksena & Bixler, 1990).

Automated facial recognition technology can detect dysmorphic facial features from two-dimensional photographs, where the object is not identifying a specific subject, but rather suggesting a list of possible syndrome-matches. The analysis process consists of five steps as described by Basel-Vanagaite et al. (2016). First, the frame of the face is located using a deep learning-based cascaded face detector (Viola & Jones, 2001). Then, within the detection frame, 130 fiducial facial points are located using similar local image detectors trained for each one of the points individually (Figure 1).The face is aligned using the fiducial facial points and then fed into an ensemble of convolutional neural networks (Li, Lin, Shen, Brand, & Hua, 2015) These networks are trained to evaluate the extent of similarity to the gestalt associated with each of a multitude of syndromes which the system is able to identify. In addition, from the anatomical points located, various local properties such as ratios of distances and local image descriptors of the face are computed. These measurements are used in combination with statistical models called Bayesian networks (Neuberg, 2003) to indicate the presence of dysmorphic features. Lastly, a mask or composite image depicting the characteristic appearance of each syndrome is created and the gestalt agreement between the test subject and each of the syndromes is visually presented using a colored heatmap (Figure 3).

This deep phenotyping technology is trained to identify specific syndromes from a patient's facial photo and may be helpful for medical professionals who work in clinical genetics (Basel-Vanagaite et al., 2016; Lumaka et al., 2016) as well as in complementing exome analysis by inferring causative genetic variants from sequencing data (Gripp, Baker, Telegrafi, & Monaghan, 2016).

In this two-phase study, we showed the specificity and sensitivity of automated facial recognitiontechnology for detection of patients with XLHED of various age, including neonates and female carriers of XLHED.

2 | PATIENTS AND METHODS

The study was divided into two phases. Phase I, called the training set phase, corresponded to the training of the XLHED patient detector tool. Phase II corresponded to the validation phase of the tool. The patients included in each phase were independent of each other. Their oral informed consent was obtained.

2.1 | Phase I: training set phase

These analyses were performed with the Facial Dysmorphology Novel Analysis software (FDNA, Inc. Boston, MA). Patients of any age and sex with a mutation in *EDA* (patients with XLHED) were investigated. Age-suitable controls collected separately by FDNA Inc. were added.

To train the system, a statistical "face detector" was used to detect a face in the image, the de-identified visual information was extracted from the images and then analyzed. Once the system was sufficiently trained to recognize the visual markers of XLHED syndrome, a classifier was deployed in the system so that any additional photo was then analyzed by all the existing classifiers (also of other syndromes) and similarities to each specific syndrome phenotype were evaluated.

The statistical power of our automated facial recognitiontechnology in distinguishing individuals affected with XLHED from the controls was evaluated with a cross-validation scheme. In this scheme, the data bulk was split randomly (multiple times) into training sets and test sets. Each set contained half of the examples (both affected and controls), and the randomization process was repeated 20 times. At each of the 20 rounds the recognition methods were independently optimized on the training set and evaluated on the test set.

2.2 | Phase II: validation phase

A single XLHED detector was developed from the facial images of the first study by incorporating all of the frontal facial images from the males with XLHED into a single training set. This detector was applied to new images of males with XLHED enrolled in one of three studies; the 2013 NFED Family Conference Study (NCT01871714) and two ongoing clinical studies being conducted by Edimer Pharmaceuticals, Inc. (NCT01775462 and NCT02099552). The NFED study enrolled 15 males with a clinical diagnosis of HED, 12 of whom had a *EDA* mutation. The age distribution in this cohort was eight children from

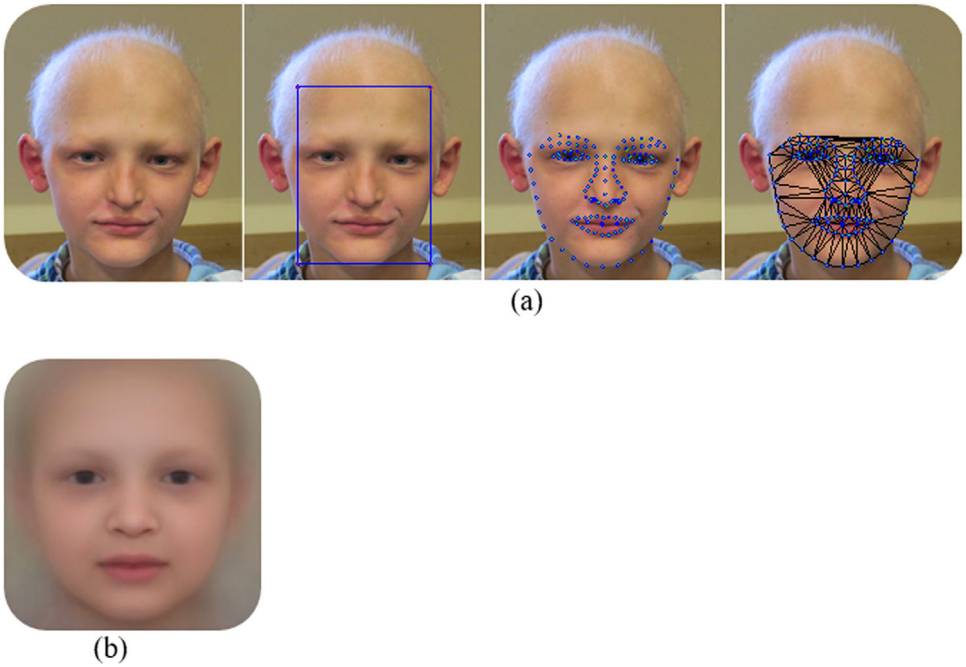

FIGURE 1 Image analysis process of the automated facial recognition technology used in this study. (a) The face is detected in the frontal image and anatomical points are automatically identified. The face is divided into multiple regions, whose appearance is analyzed. (b) Lastly, a mask depicting the characteristic appearance of each syndrome is created. [Color figure can be viewed at wileyonlinelibrary.com]

ages 1 to 10 years and seven age 11 years or older. Clinical trial NCT01775462 collected images from five newborn males with genotype-confirmed XLHED, and clinical trial NCT02099552 collected images from ten males with XLHED and an *EDA* mutation. The total number of images submitted for analysis was 30, with 27 confirmed as XLHED.

In addition, three sets of images were consolidated for test validation in genotype-confirmed XLHED carrier females (total of 31 individuals): four images of females carrying XLHED mutations were obtained in the clinical trial NCT02099552, 22 images of XLHED carrier females were contributed by the Necker Reference center for genodermatoses, and five XLHED images of carrier females were obtained as part of a study of adult women at risk for XLHED who enrolled at the 2013 NFED FC (NCT01871714). All these women were heterozygous for an *EDA* mutation.

Lastly, images from patients with other ED syndromes were collected and analyzed. They included male and female HED patients with mutations in downstream genes: that is *EDAR*, *EDARADD*, or *IKBKG* (*NEMO*). Patients carrying *IKBKG* mutations presented with HED associated to immune deficiency (MIM#300291). Patients with ED syndromes caused by mutations in the *TP63* gene were included: ankyloblepharon-ectodermal defects-cleft lip and palate (AEC or Hay–Wells syndrome, MIM#106260) and the Rapp–Hodgkin syndrome (MIM#129400), Ectrodactyly, ED, and cleft lip/palate syndrome 3 (EEC3, MIM#604292), and split-hand foot malformation (MIM#603273).

For each image analyzed, the automated facial recognition technology determined an XLHED score. The higher the score, the more features typical for XLHED are present, with a theoretical value of zero representing no features related to XLHED. Dual test score cutoffs were assessed: (1) a screening threshold score of 3.88 from the control population representing a cutoff for 99% specificity; and (2) a screening threshold cutoff value of 2.0 was selected based on visual inspection of the data for the entire dataset. In addition, the images were tested for 209 other genetic syndromes included in our automated facial recognition system. The level of similarity of the facial images to these syndromes was ranked from highest to lowest. The results are reported computing statistic of the ROC curve to measure classification success.

3 | RESULTS

3.1 | Phase I

Three sets of images were used to evaluate the technological feasibility of identifying the XLHED phenotype of various age groups: (i) 1–10 years ($n = 83$, photographs from 64 individuals); (ii) above 11 years ($n = 46$ photographs from 42 individuals); and (iii) under 1 month ($n = 38$ photographs from 30 individuals, 27 frontal, and 11 angled). Age 11 years was used as the cutoff for adult dentition.

The pediatric and adult XLHED cohorts (sets i and ii, respectively) were assessed from high quality frontal facial photographs obtained under controlled settings. The XLHED neonate photos (set iii) were provided by patient families often years to decades after the birth of the patient and were of variable quality. These images were heterogeneous with regards to pose; 27 of these images were

TABLE 1 Training set phase: sensitivity detection

Tested group	AUC	EER	Sensitivity at 95% specificity	Specificity at 99% sensitivity	Specificity at 95% sensitivity	Specificity at 90% sensitivity	Specificity at 75% sensitivity	Specificity at 50% sensitivity
Adults	0.99	0.02	98%	92% FP = 1	98% FP = 0	100% FP = 0	100% FP = 0	100% FP = 0
Children	0.99	0.03	97%	81% FP = 2	95% FP = 1	98% FP = 0	100% FP = 0	100% FP = 0
Neonates (frontal view)	0.98	5%	95%	84% FP = 3	86% FP = 2	97% FP = 0	100% FP = 0	100% FP = 0
Neonates (angle view)	1.00	0%	100%	100% FP = 0	100% FP = 0	100% FP = 0	100% FP = 0	100% FP = 0

AUC, area under curve; EER, equal error rate; FP, false positives (in the cross-validation splits).

identified as full frontal images and 11 of these images were taken from an angle. Subsequently, these images were compared to the appropriately angled control image set.

Age-suitable controls were added as follows: (i) a set of 285 male unaffected children bringing the control total to 292; (ii) A set of 204 unaffected males 11 years and up for a total of 218 controls; and (iii) a set of 207 unaffected male and female neonates, of which 33 were represented in frontal images and 174 were represented in angled images. For better understanding of the results, we reported results obtained with and without these additional controls.

Supplementary Figure S1 depicts the age distribution of the children and adults in both the patient group and the control group constituting the training set. The exact ages of controls in the newborn group were also unknown, but were generally homogeneous in nature (all images were taken at the maternity wards within the first few days after birth). Therefore, the newborn age distribution was not presented in the charts above.

The three age groups of XHLED images were assessed for sensitivity of detection at various levels of specificity and vice versa (Table 1). Independent of patient age, the automated facial recognition system was successful in distinguishing XLHED male subjects from controls in phase 1 (Figure S2). As a potential screening tool, analyses confirmed that specificities of 99–100% could be obtained with sensitivities of 75% in all age groups. The Area Under Curve (AUC) of the ROC curve statistics (which reports an aggregated score of the sensitivity-specificity trade-off), and the Equal Error Rate (EER) statistics (which is the common error rate when one sets the acceptance threshold such that the false acceptance rate and the false rejection rate are equal) were also reported.

3.2 | Phase II

The XLHED detection scores for affected males and carrier females from the second phase of this study are reported Table 2. The XLHED male cohort had a broad spectrum of *EDA* mutations but there was no apparent association of the mutation and the XLHED test score 2; the technology was 100% accurate for each case. All 30 male individuals, including the three with a clinical diagnosis that tested negative for *EDA* mutations, scored above the XLHED threshold value of 3.88 and prompted XLHED as the first ranked possible diagnosis among all listed syndromes.

The detection score was lower for carrier females. Dropping the XLHED threshold value from 3.88 to 2.0 increased sensitivity from 42% to 65%, while maintaining specificity >99%. The FDNA system prompted XLHED as the first ranked potential diagnosis in 55% of these individuals (17/31). As expected, carrier females had lower

TABLE 2 Facial XLHED detection scores of the validation phase

Image source	Sex	N	Age range	XLHED score range	XLHED scores >3.88	XLHED scores >2.00	XLHED ranked #1
2013 NFED FC	M	12	4–30 years	7.1–14.4	12/12 (100%)	12/12 (100%)	12/12 (100%)
NCT01775462	M	5	2–20 days	4.3–12.1	5/5 (100%)	5/5 (100%)	5/5 (100%)
NCT02099552	M	10	1–3 years	4.8–18.2	10/10 (100%)	10/10 (100%)	10/10 (100%)
XLHED totals	M	27	2 days–30 years	4.3–18.2	27/27 (100%)	27/27 (100%)	27/27 (100%)
2013 NFED FC	F	5	30–44 years	0.1–4.1	1/5 (20%)	1/5 (20%)	1/5 (20%)
Necker	F	22	5–73 years	0.6–13.5	11/22 (50%)	16/22 (73%)	14/22 m(64%)
NCT02099552	F	4	2–3 years	1.6–5.4	1/4 (25%)	3/4 (75%)	2/4 (50%)
XLHED totals	F	31	2–73 years	0.1–13.5	13/31 (42%)	20/31 (65%)	17/31 (55%)

F, female; M, male, N, number of patients tested.

TABLE 3 Facial XLHED detection scores within multigenerational families

Family # (mutation)	Affected (age in years)	XLHED score	Affected (age in years)	XLHED score	Affected (age in years)	XLHED score	Affected (age in years)	XLHED score
1 (p.M1R)	Mother (30)	5.5	Daughter (6)	5.8				
2 (c.572-590del18)	Mother (32)	0.6	Daughter (10)	1.7				
3 (del ex2)	Mother (36)	5.2	Daughter (14)	13.5				
4 (p.L266R)	Mother (73)	1.8	Daughter (42)	2.9	Daughter (43)	3.6	Grand daughter (6)	1.8
5 (p.R244*)	Mother (47)	3.7	Daughter (19)	2.9				

scores than affected males (Figure S3). The Necker images consisted of five sets of multigenerational frontal images that were confirmed XLHED carriers. Results showed a trend toward a higher detection score within the XLHED carriers with null mutations, for example, families 1, 3, and 5 (Table 3).

The testing of the automated facial recognition algorithm that was developed from images of XLHED male patients (*EDA* mutations) recognized both male and female HED patients with mutations in downstream genes including *EDAR*, *EDARADD*, and *IKBKG* (*NEMO*) (Supplemental Online Table S1). Male HED patients with *WNT10A* mutations also scored high with the XLHED-derived algorithm, but this was not true for the small number of *WNT10A* HED females. Unexpectedly, the six patients with p63 mutations, presenting an ED phenotype very different from the more common HED, all had facial features recognized by the XLHED-derived algorithm.

4 | DISCUSSION

The results from both phases demonstrated that our automated facial recognition technology was successful in recognizing the XLHED phenotype. The system was able to identify affected males of all ages, carriers who were variably affected, and it picked up on the facial resemblance in other ED syndromes. While a dermatologist or a geneticist may recognize ED in adults in most of the cases, the overlap between the anhidrotic phenotypes, that is, caused by *EDA*, *EDAR*, or *EDARADD* mutations, does not allow prediction of the disease-causing gene. The phenotype is less pronounced in infants, and in our experience many centers propose to sequence a panel of genes to establish a genetic diagnosis. In Necker Hospital's center (more than 150 EDA patients), the clinicians reach a genotype-phenotype correlation of around 80%.

Facial analysis technology as a sensitive and specific screening modality could be used to expedite diagnoses that in turn would lead to patients getting earlier and more effective medical treatment. It could also be useful for family planning purposes, as it may identify carriers who are not aware of their condition. Moreover, this approach can be useful for obstetricians, pediatricians, neonatologists in medical centers in which no geneticist or dermatologist is present. The automated facial recognition technology as a screening tool can also be helpful in countries where syndrome experts are rare and where the disease is associated with early death related to inability to regulate body temperature. It might also decrease the frequency of inappropriate gene sequencing.

The classifiers constructed from the data of phase I allowed us to assess the relative importance of the facial regions and attributes in the characteristic facial appearance of XLHED (Figure 2). The association of a feature with XLHED does not necessarily mean that the dysmorphic feature exists in its medical definition sense, but rather that it can be mildly expressed in the face and still be informative.

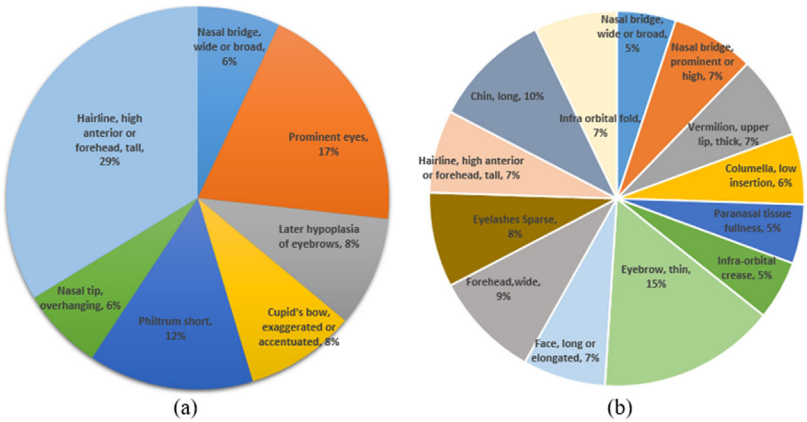

FIGURE 2 XLHED-associated facial attributes. The automated facial recognition system identified the reported facial attributes as most associated with XLHED images from the (a) child group; and (b) adult group. [Color figure can be viewed at wileyonlinelibrary.com]

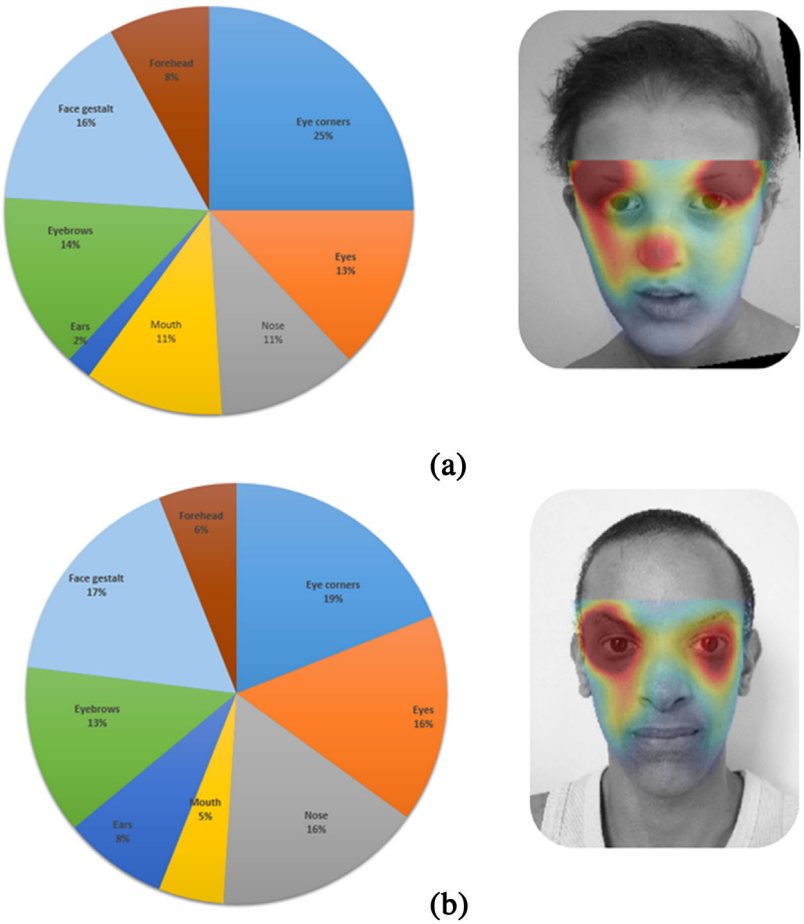

FIGURE 3 Heatmap of relative importance of various facial regions. The most distinguishable regions of the XLHED phenotype as drawn over a sample of an XLHED patient photo on the (a) Child group and (b) adult group. These results from local appearance models are built per-region and are then integrated as the gestalt component of the automated facial recognition system. Local appearance patches extracted from these regions contributed the most to the successful detection of XLHED phenotypes.

In addition to the morphometric approach, local image information is integrated in order to provide the appearance or gestalt description of the face. This process enables evaluation of the probability of an XLHED diagnosis directly for each part of the face and/or for the entire face. Moreover, this probability can be provided in an alternative manner without relying on the detection of specific dysmorphic facial features. This is the reason why even syndromes where a cleft lip is present may not affect the gestalt analysis. Figure 3 depicts the most distinguishable regions of the XLHED phenotype, drawn over sample faces, and the relative importance of various facial regions.

Three-dimensional analysis is another possible screening technology to be used for this purpose. Its scans hold additional information, also face detection, but the encoding and classification methods are different. Three-dimensional analysis requires special capturing equipment and analytical software which makes three-dimensional imaging research less accessible. A comparison of our automated facial recognition technology with three-dimensional imaging was not within the scope of this paper.

It is important to note that the results displayed in Table 2 for the set of neonates (angle view) may contain a significant bias due to the heterogeneous nature of the positive XLHED images used in this study, in terms of image quality and pose (i.e., the range of angles used), whereas the control set was fairly homogenous as its images were taken in similar settings, quality, and pose. Obtaining images of affected and controls from similar sources could allow us to obtain more accurate results.

Detection of female *EDA* mutation carriers is an important screening step in order to further support early diagnosis of affected male newborns. In the limited 2013 NFED cohort, there were five women of child-bearing age who were at risk for XLHED based on HED family history but tested *EDA*-mutation negative—in addition to five healthy adult women as controls without known ED risk (Table 1). In the *EDA*-mutation negative cohort, only one subject had an XLHED score $\geq$2.0 and this image was ranked first for XLHED. For this subject, a germline mutation might explain the full phenotype in the child and both the negative FDNA and genetic testing on blood DNA. All five images from controls scored <1.0 and none ranked in the high range.

In conclusion, the FDNA recognition tool has the potential to be an effective XLHED screening tool at any age. A larger study is required to determine the real value of this screening assessment and false positive/false negative rates.

5 | CONFLICTS OF INTEREST

K.H. was the medical director of Edimer Inc. at the time this study was conducted, N.K. is an employee of Edimer Inc,. L.W. is a co-founder of FDNA Inc., M.O is a research associate at FDNA Inc. There is no conflict of interest to declare for S.HR., H.S., E.N., K.O., S.W., C.B, and D.G.

ACKNOWLEDGMENT

We are indebted to the patient associations of all countries where subject photos were obtained.

REFERENCES

Basel-Vanagaite, L., Wolf, L., Orin, M., Larizza, L., Gervasini, C., Krantz, I. D., & Deardoff, M. A. (2016). Recognition of the Cornelia de Lange syndrome phenotype with facial dysmorphology novel analysis. *Clinical Genetics*, *89*(5), 557–563.

Cambiaghi, S., Restano, L., Pääkkönen, K., Caputo, R., & Kere, J. (2000). Clinical findings in mosaic carriers of hypohidrotic ectodermal dysplasia. *Archives of Dermatology*, *136*, 217–224.

Cluzeau, C., Hadj-Rabia, S., Jambou, M., Mansour, S., Guigue, P., Masmoudi, S., . . . Smahi, A. (2011). Only four genes (EDA1, EDAR, EDARADD, and WNT10A) account for 90% of hypohidrotic/anhidrotic ectodermal dysplasia cases. *Human Mutation*, *32*, 70–72.

Fete, M., Hermann, J., Behrens, J., & Huttner, K. M. (2014). X-linked hypohidrotic ectodermal dysplasia (XLHED): Clinical and diagnostic insights from an international patient registry. *American Journal of Medical Genetics Part A 164A*:2437–2442.

Goodwin, A. F., Larson, J. R., Jones, K. B., Liberton, D. K., Landan, M., Wang, Z., . . . Klein, O. D. (2014). Craniofacial morphometric analysis of individuals with X-linked hypohidrotic ectodermal dysplasia. *Molecular Genetics & Genomic Medicine*, *2*, 422–429.

Gripp, K. W., Baker, L., Telegrafi, A., & Monaghan, K. G. (2016). The role of objective facial analysis using FDNA in making diagnoses following whole exome analysis. Report of two patients with mutations in the BAF complex genes. *American Journal of Medical Genetics Part A*, *9999A*, 1–9.

Li, H., Lin, Z., Shen, X., Brand, Jt., & Hua, G., (2015). A convolutional neural network cascade for face detection. *In Proc. IEEE Conference on Computer Vision and Pattern Recognition*. 5325–5334.

Lumaka, A., Lukoo, R., Mubungu, G., Lumpala, P., Mbayabo, G., Mupuala, A., . . . Devriendt, K. (2016). Williams-Beuren syndrome: Pitfalls for diagnosis in limited resources setting. *Clinical Case Reports*, *4*, 294–297.

Neuberg, L. G. (2003). Causality, models reasoning and inference by Judea Pearl (book review). *Econometric Theory*, *19*, 675–685.

Saksena, S. S., & Bixler, D. (1990). Facial morphometrics in the identification of gene carriers of X-linked hypohidrotic ectodermal dysplasia. *American Journal of Medical Genetics*, *35*, 105–114.

Schneider, H., Hammersen, J., Preisler-Adams, S., Huttner, K., Rascher, W., & Bohring, A. (2011). Sweating ability and genotype in individuals with X-linked hypohidrotic ectodermal dysplasia. *Journal of Medical Genetics 48*, 426–432.

Viola, P. A., & Jones, M. J. (2001). Rapid object detection using a boosted cascade of simple features. *Computer Vision and Pattern Recognition, In Proc. IEEE Conference on Computer Vision and Pattern Recognition*, 1–9.

Visinoni, A. F., Lisboa-Costa, T., Pagnan, N. A., & Chautard-Freire-Maia, E. A. (2009). Ectodermal dysplasias: Clinical and molecular review. *American Journal of Medical Genetics*, *149A*, 1980–2002.

Wisniewski, S. A., & Trzeciak, W. H. (2012). A rare heterozygous TRAF6 variant is associated with hypohidrotic ectodermal dysplasia. *British Journal of Dermatology*, *166*, 1353–1356.

SUPPORTING INFORMATION

Additional Supporting Information may be found online in the supporting information tab for this article.

How to cite this article: Hadj-Rabia S, Schneider H, Navarro E, et al. Automatic recognition of the XLHED phenotype from facial images. *Am J Med Genet Part A*. 2017;173A:2408–2414.
https://doi.org/10.1002/ajmg.a.38343